

Fractal analysis of chaotic classical scattering in a cut-circle billiard with two openings

Suhan Ree*

Department of Industrial Information, Kongju National University, Yesan-Up, Yesan-Gun, Chungnam 340-800, South Korea

L. E. Reichl

Center for Studies in Statistical Mechanics and Complex Systems, The University of Texas at Austin, Austin, Texas 78712

(Received 13 February 2002; published 14 May 2002)

We investigate the fractal behavior of the transmission of a classical particle through a circular billiard with a straight cut and two openings. As the size of the cut varies, the phase space of the closed billiard shows a full range of dynamical behavior, including integrable behavior, soft chaos (mixed phase space), and hard chaos (ergodic and mixing). For an open billiard, we numerically find the exit opening as a function of the incident angle. When the billiard is chaotic, the result shows self-similarity and infinite complexity. We calculate the fractal dimension of this structure using a box-counting method when two parameters, the size of the cut and the size of the openings, are varied.

DOI: 10.1103/PhysRevE.65.055205

PACS number(s): 05.45.Df, 05.45.Pq, 73.23.Ad

Billiards have special advantages for studying classical chaos and its manifestations in semiclassical and quantum mechanics [1]. The shape of the walls largely determines dynamical behavior, and therefore numerical calculations are relatively easy. Classically the dynamics of billiard systems exhibits one of the three types of behavior: (1) integrable (regular), (2) *soft chaos* (characterized by mixed phase spaces that have both regular and chaotic regions), and (3) *hard chaos* (ergodic and mixing) [2]. Billiards that exhibit chaotic behavior caused by the walls have been built in the laboratory. One example is the two-dimensional (2D) semiconductor heterostructure in the *ballistic* regime. In these nanoscale structures, the magnetoconductance through the structure fluctuates in different ways, depending on whether the classical dynamics of the billiard is regular or chaotic [3].

Fractal behavior has been observed in several aspects of billiard dynamics. In Refs. [4–8], quantum conductance fluctuations are shown to exhibit self-similarity up to a certain scale, and it is argued that this self-similar structure is induced by fractal structures in the underlying classical mixed phase space. The scattering of classical particles in open billiards has also been shown to have fractal behavior [9–11], for example, in the number of collisions with the walls as a function of the incident angle.

In this Rapid Communication, we numerically investigate the fractal dimension of the transmission of a classical particle through a circular billiard with a straight cut and two openings (see Fig. 1). There are five parameters that affect the dynamics: (1) the maximum width W in the direction perpendicular to the cut, (2) the radius R of the circle, (3) the angular width Δ of the openings, (4) the orientation angle Ω of the cut relative to the first opening, and (5) the position of the second opening relative to the first opening as measured by the angle γ . We can scale the width W by R so $w \equiv W/R$, and thereby reduce the number of independent parameters to four: w , Δ , Ω , and γ . For all subsequent discussions, we set $\Omega = 135^\circ$ and $\gamma = 270^\circ$. This leaves two param-

eters that control the system, w and Δ . When there is no opening ($\Delta = 0$), w is the only parameter that controls the dynamical behavior of this cut-circle billiard. In Ref. [12], it has been proved that the phase space is mixed (soft chaos) when $0 < w < 1$, and the phase space is fully chaotic (hard chaos) when $1 < w < 2$. The system is integrable when $w = 1$ and 2 . Numerical studies of classical chaos for the closed cut-circle billiard and its quantum manifestations, and the Landauer-Büttiker conductance for the quantum cut-circle billiard with two conical leads have been discussed in Refs. [13] and [14], respectively.

We inject a particle from the center of the opening I (see Fig. 1) with an angle ϕ (“the incident angle,” $-\pi/2 < \phi < \pi/2$). By following the trajectories for this initial condition, one can calculate several quantities, including the num-

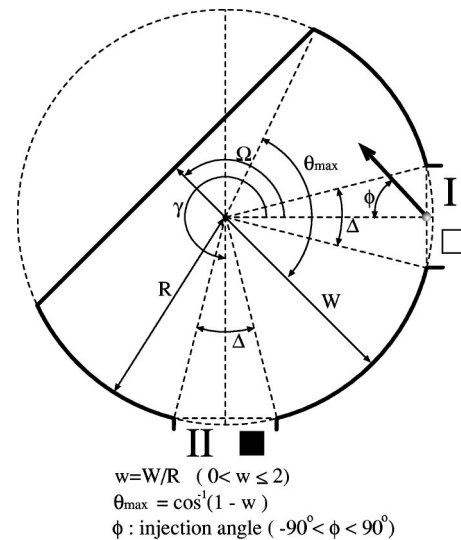


FIG. 1. The geometry of the system. A cut-circle billiard has two openings, I and II. The size of the straight cut is given by the width W . The width of two openings is Δ , and the position of the cut and the second opening, Ω and γ , are measured from the first opening. A particle is injected from the center of the opening I with an angle ϕ .

*Electronic address: suhan@kongju.ac.kr

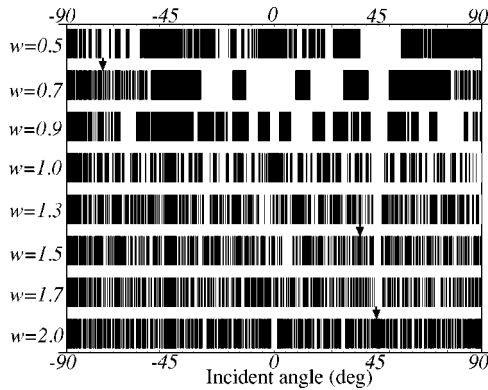


FIG. 2. Graphs of the exit opening vs the incident angle ϕ . Black bars represent transmission windows, and white bars represent reflection windows. The resolution $\Delta\phi$ is $\pi/5000$. As w is varied from 0.5 to 2, we observe increased complexities.

ber of collisions before the particle exits, the length of the path, the opening from which the particle exits (“the exit opening”), and also the statistics of this data. Such quantities have been computed for the 2D cross junction [10] and the 2D ripple channel [11]. Here we focus on the simplest outcome, the incident angle ϕ vs the exit opening, for given Δ and w . From the deterministic classical dynamics, we can obtain a function $T^{\Delta,w}$, which maps the incident angle in opening I to one of the two values, I and II, depending on whether the particle exits from opening I (reflection) or opening II (transmission). For some Δ and w values, $T^{\Delta,w}$ has an infinitely fine structure. We will represent $T^{\Delta,w}$ by means of a graph with black and white bars. A bar is black for a range of ϕ in which the particle transmits (exits from II), and a bar is white for a range of ϕ in which the particle reflects (exits from I). There are series of “transmission windows” (black) separated by “reflection windows” (white), in the range, $-\pi/2 < \phi < \pi/2$. The resolution $\Delta\phi$ of ϕ is given by

$$\Delta\phi \equiv \frac{\pi}{N_p}, \quad (1)$$

where N_p is the number of incident angles. The incident angles $\{\phi_i | i=1, \dots, N_p\}$ are uniformly distributed in the given range,

$$\phi_i = -\frac{\pi}{2} + \frac{i\pi}{N_p+1} \quad (i=1, \dots, N_p). \quad (2)$$

When the size of a transmission (or reflection) window is smaller than $\Delta\phi$, there is a chance of missing it in numerical simulations. Thus, we can only see the structure up to a given resolution of ϕ . When $T^{\Delta,w}$ has an infinitely fine structure, the number of windows found numerically will increase as N_p increases. This relationship between the number of windows found and N_p will later be used to calculate the fractal dimension—a quantitative measure of this infinite complexity.

In Fig. 2, the behavior of $T^{\Delta,w}(\phi)$, calculated numerically, is shown for several w values when $\Delta = 10^\circ$. We ob-

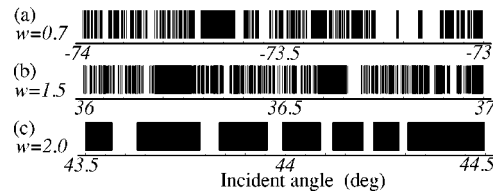


FIG. 3. Zoomed-in graphs for three different cases. In Fig. 2, these cases are pointed by arrows, and they all have the range of one degree. (a) $w=0.7$ (soft chaos), (b) $w=1.5$ (hard chaos), and (c) $w=2$ (regular).

serve some big transmission windows, which are called *geometrical channels* [10], and they play an important role in real systems because trajectories in these windows usually have only few collisions with the boundary. We also observe that, for cases of soft chaos (when $w < 1$), regions of big windows and regions of small windows coexist. On the other hand, for cases of hard chaos (when $1 < w < 2$), very small windows tend to be populated throughout the whole region. Regular cases (when $w = 1, 2$) also look complex at first glance. In Fig. 3, we zoom in for three different cases, and we can clearly see the difference. When $w=0.7$ [Fig. 3(a)] and $w=1.5$ [Fig. 3(b)], we see smaller windows again coexisting with larger windows. But when $w=2$ [Fig. 3(c)], we no longer see small windows. In general, the larger the window, the less the number of collisions with the boundary. This fractal structure is a signature of chaos.

In Fig. 4, we examine the behavior of the transmission when $w=1.01$ (nearly integrable). In Fig. 4(a), we look at a small interval of size 10^{-2} (rad). In Fig. 4(b), we magnify a small interval of Fig. 4(a) by a factor of 100. Similarly, in Fig. 4(c) [4(d)], we magnify a small interval of Fig. 4(b) [4(c)] by a factor of 100. We still observe windows much smaller than 10^{-8} (rad). Figure 4(e) shows the trajectory with the incident angle very close to the center of this region (ϕ is $4.385\,942\,4^\circ$). The injected particle bounces close to the (1,2) orbit for a long time (about 150 bounces), and finally exits to the opening II after 207 collisions with the walls. We expect that all trajectories associated with this region stay close to the (1,2) orbit for many bounces [15] For this reason, an orbit like this (1,2) orbit is called *the strange repeller* [10,16,17]. These strange repellers seem to make transmission windows around them infinitely small, and they cause this infinite complexity. For cases with hard chaos, there exist many unstable periodic orbits acting as strange repellers, while for integrable cases there is no unstable orbit. For cases with soft chaos, the positions of the initial conditions relative to the mixed phase spaces determine the behavior of trajectories.

We have so far observed qualitative aspects of self-similarity. Now we focus on a quantitative analysis of this observed complexity. We can regard these transmission windows as a set of ranges embedded inside an one-dimensional set, $(-\pi/2, \pi/2)$. One useful measure describing such a self-similar set is the fractal dimension [18]. But, unlike common fractals such as the Cantor set, this set has nonzero Lebesgue measure, and, as a result, the fractal dimension of this set is the same as that of the underlying space, which is one. This

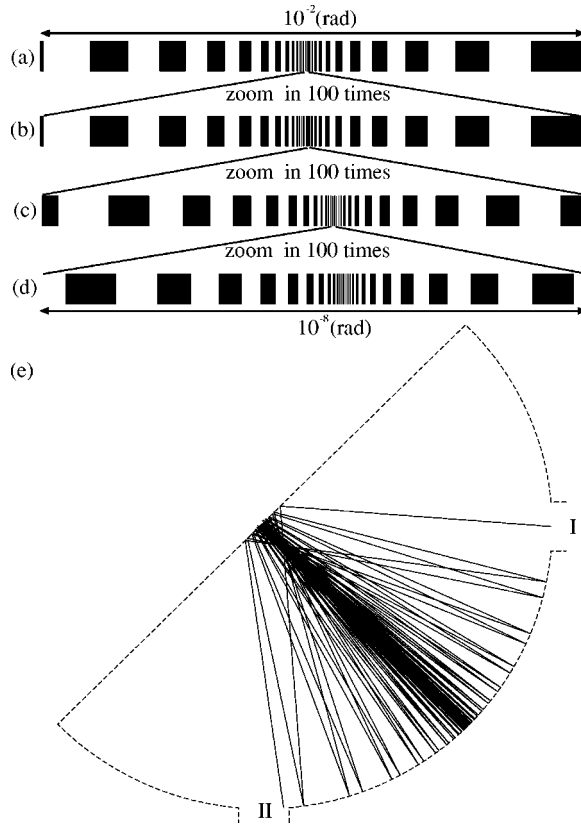


FIG. 4. Self-similarity when $w = 1.01$. We zoom in by 100 times for each successive range: (a) $4.099\,461\,5^\circ < \phi < 4.672\,419\,2^\circ$, (b) $4.383\,075\,6^\circ < \phi < 4.388\,805\,1^\circ$, (c) $4.385\,911\,7^\circ < \phi < 4.385\,969\,0^\circ$, (d) $4.385\,942\,1^\circ < \phi < 4.385\,942\,6^\circ$. (e) The trajectory when the incident angle ϕ is given at $4.385\,942\,4^\circ$. The particle is injected at the center of the opening I, and exits from the opening II.

kind of fractals are called *fat fractals* [19–21]. (And fractals with zero Lebesgue measure are called *thin fractals* instead.) Several scaling exponents are defined for fat fractals, but since the boundary of a fat fractal is a thin fractal [9], we will calculate the fractal dimension of the boundary of $T^{\Delta,w}$, $\partial T^{\Delta,w}$, instead. In other words, our quantitative measure of self-similarity in our system is the fractal dimension of the set of boundaries of transmission windows. Here the fractal dimension d_f will be a continuous function of Δ and w . For calculations of the fractal dimension, a box-counting method is simple to apply. From Eq. (1), there are N_P boxes of width $\Delta\phi$ for a given resolution of ϕ . [Note that the numerical error should be much smaller than $\Delta\phi$. In our numerical calculations for d_f , double-precision numbers with 15 significant digits were used, and $\Delta\phi$ was at least 10^{-7} (rad), to get reliable results.] The number of boxes containing the set $\partial T^{\Delta,w}$ is represented by the number of transmission windows, N_B , for given N_P . (Precisely the number is $2N_B$, but a constant factor can be ignored for calculations of the fractal dimension.) The fractal dimension d_f for given Δ and w is

$$d_f = \lim_{N_P \rightarrow \infty} \frac{\log_{10} N_B}{\log_{10} N_P}. \quad (3)$$

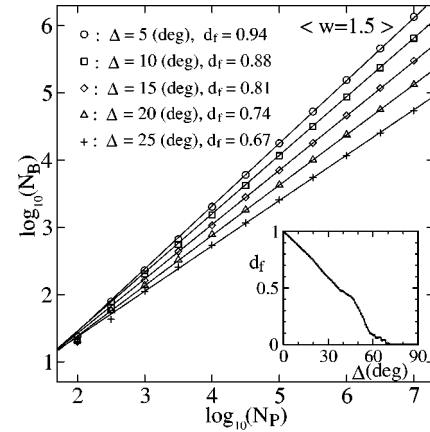


FIG. 5. Graphs of $\log_{10} N_P$ vs $\log_{10} N_B$ when $w = 1.5$ and the opening size Δ is varied. N_P is the number of total boxes and N_B is the number of transmission windows for the given resolution. The inset shows how the fractal dimension d_f changes as Δ varies.

In Fig. 5, we fix the width w at 1.5 (hard chaos), and vary the opening size, Δ . Here we calculate d_f by finding the slope of a line fitting the linear part of the graph of $\log_{10} N_B$ vs $\log_{10} N_P$ using the ordinary least-square fit. As Δ approaches zero, the size of transmission windows becomes infinitely small, and, as a result, d_f approaches one (it may not approach one in other cases). Also as Δ increases, d_f decreases and eventually reaches zero. Thus for $w = 1.5$, when $\Delta \sim 68^\circ$, d_f becomes zero and the scattering dynamics no longer exhibits infinite complexity. This result implies that, for this case, the global chaos of the closed billiard disappears in classical mechanics when the opening size reaches a certain critical value.

In Fig. 6, we fix the opening size Δ at 5° , and vary the width w . We observe that there is a clear distinction between soft and hard chaotic regions in the graph of d_f vs w . For regular cases ($w = 1, 2$), d_f is zero. In the soft chaotic region ($w < 1$), d_f fluctuates with w , but in the hard chaotic region ($1 < w < 2$), it has a smooth plateau. In the soft chaotic region, the fluctuation occurs due to nonuniform mixed phase spaces, since relative positions of openings relative to phase-

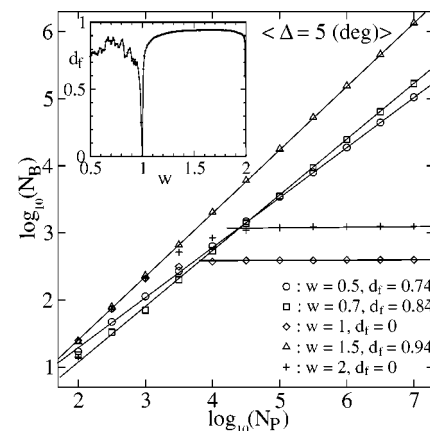


FIG. 6. Graphs of $\log_{10} N_P$ vs $\log_{10} N_B$ when the opening size $\Delta = 5^\circ$ and w is varied. The inset shows how the fractal dimension d_f changes as w varies.

space structures varies as w changes. (We can do the same fractal analysis on a set of singularities of a graph of the number of collisions N_S vs the incident angle ϕ . But d_f values are the same as those from Figs. 5 and 6, because in chaotic regions N_S will be proportional to N_B for given N_P .)

To summarize, we have numerically observed the self-similarities and infinitely hierarchical structures in the transmission of a classical particle that scatters through a chaotic billiard. This fractality comes from the chaotic nature of the underlying closed billiard, and also from the presence of openings. The graph used for the fractal analysis is a fat fractal, and boundaries of our fat-fractal sets have been used for the calculations of the fractal dimension. When the open-

ing size approaches zero, the fractal dimension approaches the highest possible value for a given billiard (one, in our example). And when the opening size reaches a certain value, the fractal dimension becomes the lowest possible value (zero, in our example). We have also observed that the behavior of the fractal dimension is different for soft and hard chaos when the parameter that controls the degree of chaos is varied.

S.R. wishes to thank Kongju National University for support of this work. L.E.R. wishes to thank the Welch Foundation, Grant No. F-1051, NSF Grant No. INT-9602971, and DOE Contract No. DE-FG03-94ER14405 for partial support of this work.

-
- [1] L.E. Reichl, *The Transition to Chaos in Conservative Classical Systems: Quantum Manifestations* (Springer-Verlag, New York, 1992).
- [2] M.C. Gutzwiller, *Chaos in Classical and Quantum Mechanics* (Springer-Verlag, New York, 1990).
- [3] C.M. Markus, A.J. Rimberg, R.M. Westerfelt, P.F. Hopkins, and A.C. Gossard, Phys. Rev. Lett. **69**, 506 (1992).
- [4] R. Ketzmerick, Phys. Rev. B **54**, 10 841 (1996).
- [5] A.S. Sachrajda, R. Ketzmerick, C. Gould, Y. Feng, P.J. Kelly, A. Delage, and Z. Wasilewski, Phys. Rev. Lett. **80**, 1948 (1998).
- [6] C.R. Tench, T.M. Fromhold, P.B. Wilkenson, M.J. Carter, R.P. Taylor, A.P. Micolich, and R. Newbury, Physica E (Amsterdam) **7**, 726 (2000).
- [7] G. Casati, I. Guarneri, and G. Maspero, Phys. Rev. Lett. **84**, 63 (2000).
- [8] B. Huckestein, R. Ketzmerick, and C.H. Lewenkopf, Phys. Rev. Lett. **84**, 5504 (2000).
- [9] B. Eckhardt, J. Phys. A **20**, 5971 (1987).
- [10] M.L. Roukes and O.L. Alerhand, Phys. Rev. Lett. **65**, 1651 (1990).
- [11] G.A. Luna-Acosta, A.A. Krokhin, M.A. Rodríguez, and P.H. Hernández-Tejeda, Phys. Rev. B **54**, 11 410 (1996).
- [12] L.A. Bunimovich, Commun. Math. Phys. **65**, 295 (1979).
- [13] S. Ree and L.E. Reichl, Phys. Rev. E **60**, 1607 (1999).
- [14] K. Fuchss, S. Ree, and L.E. Reichl, Phys. Rev. E **63**, 016214 (2000).
- [15] A closed orbit (1,2) is a two-bounce periodic orbit, and lies on the axis that is perpendicularly placed at the center of the cut. It is unstable when $1 < w < 2$, stable when $0 < w < 0.5$ or $0.5 < w < 1$, and marginally stable when $w = 0.5, 1, 2$.
- [16] V.I. Kozub, Europhys. Lett. **18**, 337 (1992).
- [17] P. Gaspard, Chaos **3**, 427 (1993).
- [18] E. Ott, *Chaos in Dynamical Systems* (Cambridge, New York, 1993).
- [19] J.D. Farmer, Phys. Rev. Lett. **55**, 351 (1985).
- [20] C. Grebogi, S.W. McDonald, E. Ott, and J.A. Yorke, Phys. Lett. **110A**, 1 (1985).
- [21] R. Eykholt and D.K. Umberger, Physica D **30**, 43 (1988).